

# Diffusion and the BFKL Pomeron

J.R. Forshaw<sup>1</sup> and P. J. Sutton<sup>2</sup>

<sup>1</sup> Department of Physics and Astronomy, University of Manchester,  
Manchester, M13 9PL, England.

<sup>2</sup> Department of Theoretical Physics, Lund University,  
Sölvegatan 14 A, S-223 62 Lund, Sweden.

## Abstract

We study the high energy behaviour of elastic scattering amplitudes within the leading logarithm approximation. In particular, we cast the amplitude in a form which allows us to study the internal dynamics of the BFKL Pomeron for general momentum transfer. We demonstrate that the momentum transfer acts as an effective infrared cut-off which ensures that the dominant contribution arises from short distance physics.

# 1. Introduction

We are interested in the study of elastic scattering in the Regge limit where  $s \gg -t$ . We might expect to be able to use the methods of perturbative QCD if the typical distances involved in the interaction are small. Whilst this may be true for some elastic scattering processes (for example, two highly virtual photons at large  $t$ ) it is certainly not the case for others (for example, a pair of protons at  $t \simeq 0$ ). It is therefore necessary to check the self consistency of a perturbative calculation by investigating the typical distances involved in the interaction. If these turn out to be large then, even if the calculation is infrared finite, there is little justification for using a perturbative approach. In this paper, we consider the elastic scattering of generic colourless states via BFKL Pomeron [1] exchange. We formulate the amplitude in such a way that we can readily identify the typical distances involved in the exchange.

For elastic scattering at  $t = 0$ , the typical transverse momenta of the gluons which constitute the Pomeron are determined primarily by the sizes of the external particles. By studying the scattering of small size objects one therefore expects that perturbative QCD is valid. However, one must also take into account the diffusion properties characteristic of the BFKL exchange, namely as one moves away in rapidity from the external particles the width of the transverse momentum distribution broadens. This means that at sufficiently high centre of mass energies one is destined to pick up a large contribution from long distance effects. It is the main purpose of this paper to demonstrate that for  $t \neq 0$ , the situation changes rather dramatically. The scale  $|t|$  effectively acts as an infrared cut-off, ensuring that the essential physics comes from the region where all the momenta are bigger than  $\sim \sqrt{-t}$ . As a by-product we derive general formulae, which are useful in computing elastic scattering amplitudes in the Regge limit.

# 2. The BFKL Pomeron

We start by recalling the results of Lipatov [2] for the solution of the BFKL equation for arbitrary momentum transfer,  $\mathbf{q}^2 = -t$ . The Pomeron is described by the universal four-point function,  $F$ , depicted in Fig.1. In terms of this function, the amplitude for scattering the colourless states  $A$  and  $B$  elastically is

$$A(s, t) = \frac{is}{(2\pi)^4} \int d^2\mathbf{k}_1 d^2\mathbf{k}_2 \Phi_A(\mathbf{k}_1, \mathbf{q}) F(y, \mathbf{k}_1, \mathbf{k}_2, \mathbf{q}) \Phi_B(\mathbf{k}_2, \mathbf{q}) . \quad (1)$$

The impact factors  $\Phi_A$  and  $\Phi_B$  determine the coupling of two gluons to the external states and we define them to contain no propagator factors (these are contained in  $F$ ). Rather than work in transverse momentum space, it is more convenient to work in the space of impact parameters. Accordingly we define

$$F(y, \mathbf{k}_1, \mathbf{k}_2, \mathbf{q}) = \frac{1}{(2\pi)^6} \int d^2\mathbf{b}_1 d^2\mathbf{b}'_1 d^2\mathbf{b}_2 d^2\mathbf{b}'_2 \left\{ e^{-i[\mathbf{k}_1 \cdot \mathbf{b}_1 + (\mathbf{q} - \mathbf{k}_1) \cdot \mathbf{b}'_1 - \mathbf{k}_2 \cdot \mathbf{b}_2 - (\mathbf{q} - \mathbf{k}_2) \cdot \mathbf{b}'_2]} f(y, \mathbf{b}_1, \mathbf{b}'_1, \mathbf{b}_2, \mathbf{b}'_2) \right\} . \quad (2)$$

For future notational convenience we denote this transformation

$$F(y, \mathbf{k}_1, \mathbf{k}_2, \mathbf{q}) = \hat{\mathbb{T}} \{ f(y, \mathbf{b}_1, \mathbf{b}'_1, \mathbf{b}_2, \mathbf{b}'_2) \} . \quad (3)$$

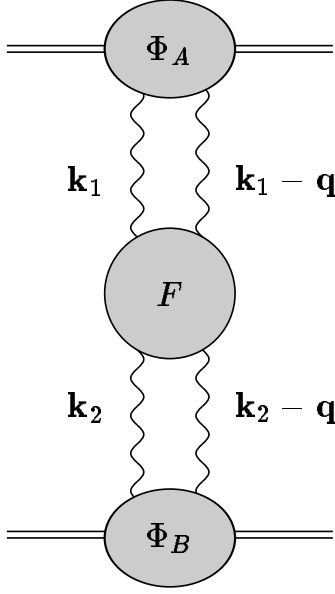


Figure 1: BFKL Pomeron exchange in elastic scattering.

Lipatov determined that

$$f(y, \mathbf{b}_1, \mathbf{b}'_1, \mathbf{b}_2, \mathbf{b}'_2) = \int_{-\infty}^{+\infty} d\nu \frac{\nu^2}{(\nu^2 + 1/4)^2} E^\nu(\mathbf{b}_1, \mathbf{b}'_1) E^{\nu*}(\mathbf{b}_2, \mathbf{b}'_2) e^{\bar{\alpha}_S \chi(\nu)y} \quad (4)$$

where  $\bar{\alpha}_S = N_c \alpha_s / \pi$  and the function  $\chi(\nu)$  is given by

$$\chi(\nu) = 2\psi(1) - \psi(1/2 + i\nu) - \psi(1/2 - i\nu) . \quad (5)$$

Here  $\psi(z)$  is the logarithmic derivative of the gamma function,  $\Gamma(z)$ . The eigenfunctions,  $E^\nu$ , are given by

$$E^\nu(\mathbf{b}_1, \mathbf{b}'_1) = \left( \frac{|\mathbf{b}_1 - \mathbf{b}'_1|}{|\mathbf{b}_1| |\mathbf{b}'_1|} \right)^{1+2i\nu} . \quad (6)$$

We have not included the contributions from non-zero conformal spin, since these vanish in the high energy limit.

It is our aim to study the internal dynamics of the BFKL Pomeron. To do this we “break” the Pomeron into two pieces, as shown in Fig.2. The procedure requires a little care, in order to account for the propagators which are present on the external legs. We utilize the following identity:

$$\tilde{F}(y, k_1, k_2, q) = \int d^2\mathbf{k} \tilde{F}(y', k_1, k, q) \tilde{F}(y - y', k, k_2, q) \quad (7)$$

where

$$\tilde{F}(y, k_1, k_2, q) = k_1(k_1 - q)k_2^*(k_2 - q)^* F(y, \mathbf{k}_1, \mathbf{k}_2, \mathbf{q}) . \quad (8)$$

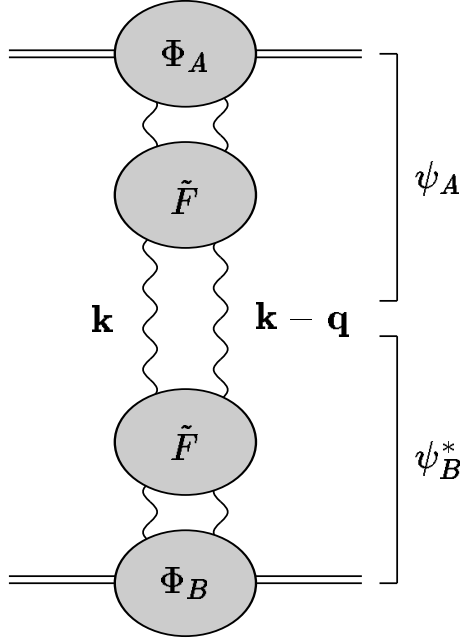


Figure 2: Elastic scattering amplitude as a convolution of the wavefunctions  $\psi_A$  and  $\psi_B^*$ .

We have introduced complex numbers to represent the transverse momentum vectors ( $k = k_x + ik_y$ ). This definition means that  $\tilde{F}$  contains the part propagators  $1/k_1^*$ ,  $1/(k_1 - q)^*$ ,  $1/k_2$  and  $1/(k_2 - q)$  on its external legs. The wavefunctions,  $\psi_{A,B}$ , contain the BFKL dynamics and are given by

$$\psi_A(y, \mathbf{k}, \mathbf{q}) = \int d^2\mathbf{k}_1 \Phi_A(\mathbf{k}_1, \mathbf{q}) \frac{\tilde{F}(y, k_1, k, q)}{k_1(k_1 - q)} \quad (9)$$

and

$$\psi_B^*(y, \mathbf{k}, \mathbf{q}) = \int d^2\mathbf{k}_2 \Phi_B(\mathbf{k}_2, \mathbf{q}) \frac{\tilde{F}(y, k, k_2, q)}{k_2^*(k_2 - q)^*}. \quad (10)$$

The scattering amplitude is then given by

$$A(s, t) = \frac{is}{(2\pi)^4} \int d^2\mathbf{k} \psi_A(y', \mathbf{k}, \mathbf{q}) \psi_B^*(y - y', \mathbf{k}, \mathbf{q}). \quad (11)$$

In terms of Lipatov's solution in impact parameter space we have

$$\frac{\tilde{F}(y, k_1, k_2, q)}{k_1(k_1 - q)} = \hat{\mathbb{T}} \left\{ (4\partial_{b_2} \partial_{b_2'}) f(y, b_1, b_1', b_2, b_2') \right\}. \quad (12)$$

Similarly,

$$\frac{\tilde{F}(y, k_1, k_2, q)}{k_2^*(k_2 - q)^*} = \hat{\mathbb{T}} \left\{ (4\partial_{b_1^*} \partial_{b_1'^*}) f(y, b_1, b_1', b_2, b_2') \right\}. \quad (13)$$

We can easily calculate  $\partial_{b_2} \partial_{b'_2} f(y, b_1, b'_1, b_2, b'_2)$  using

$$\partial_{b_2} \partial_{b'_2} E^{\nu*}(\mathbf{b}_2, \mathbf{b}'_2) = \frac{(\nu^2 + 1/4)}{(b_2 - b'_2)^2} E^{\nu*}(\mathbf{b}_2, \mathbf{b}'_2). \quad (14)$$

We thus have

$$\frac{\tilde{F}(y, k_1, k_2, q)}{k_1(k_1 - q)} = \hat{\Gamma} \left\{ \int_{-\infty}^{+\infty} d\nu \frac{4\nu^2}{(\nu^2 + 1/4)} \frac{E^\nu(\mathbf{b}_1, \mathbf{b}'_1) E^{\nu*}(\mathbf{b}_2, \mathbf{b}'_2)}{(b_2 - b'_2)^2} e^{\bar{\alpha}_{S\chi(\nu)y}} \right\}. \quad (15)$$

For our purposes it is beneficial to work in terms of the momentum transfer,  $\mathbf{q}$ , and size,  $\mathbf{b}$ . Transforming to this mixed representation, we define the new wavefunctions:

$$\Psi_A(y, \mathbf{b}, \mathbf{q}) = \int \frac{d^2\mathbf{k}}{2\pi} e^{-i\mathbf{k}\cdot\mathbf{b}} \psi_A(y, \mathbf{k}, \mathbf{q}) \quad (16)$$

and

$$\Psi_B^*(y, \mathbf{b}, \mathbf{q}) = \int \frac{d^2\mathbf{k}}{2\pi} e^{+i\mathbf{k}\cdot\mathbf{b}} \psi_B^*(y, \mathbf{k}, \mathbf{q}). \quad (17)$$

The scattering amplitude is now given by

$$A(s, t) = \frac{is}{(2\pi)^4} \int d^2\mathbf{b} \Psi_A(y', \mathbf{b}, \mathbf{q}) \Psi_B^*(y - y', \mathbf{b}, \mathbf{q}). \quad (18)$$

By evaluating these wavefunctions we are able to compute the probability for finding the Pomeron with size  $\mathbf{b}$  at rapidity  $y'$ .

To this end, we shall proceed to compute the wavefunction,  $\Psi_A$ . Using (9,15,16) we obtain

$$\Psi_A(y, \mathbf{b}, \mathbf{q}) = \frac{1}{(2\pi)^6} \int d\nu \frac{4\nu^2}{(\nu^2 + 1/4)} e^{\bar{\alpha}_{S\chi(\nu)y}} V_\nu^A(\mathbf{q}) W_\nu(\mathbf{b}, \mathbf{q}) \quad (19)$$

where

$$V_\nu^A(\mathbf{q}) = \int d^2\mathbf{k}_1 d^2\mathbf{b}_1 d^2\mathbf{b}'_1 e^{-i(\mathbf{k}_1\cdot\mathbf{b}_1 + (\mathbf{q}-\mathbf{k}_1)\cdot\mathbf{b}'_1)} \Phi_A(\mathbf{k}_1, \mathbf{q}) E^\nu(\mathbf{b}_1, \mathbf{b}'_1) \quad (20)$$

and

$$W_\nu(\mathbf{b}, \mathbf{q}) = \int \frac{d^2\mathbf{k}}{2\pi} d^2\mathbf{b}_2 d^2\mathbf{b}'_2 e^{-i(\mathbf{k}\cdot\mathbf{b} - \mathbf{k}\cdot\mathbf{b}_2 - (\mathbf{q}-\mathbf{k})\cdot\mathbf{b}'_2)} \frac{E^{\nu*}(\mathbf{b}_2, \mathbf{b}'_2)}{(b_2 - b'_2)^2}. \quad (21)$$

All of the dependence on the impact parameter  $\Phi_A(\mathbf{k}_1, \mathbf{q})$  is contained within the function  $V_\nu^A(\mathbf{q})$ . We proceed to calculate  $W_\nu(\mathbf{b}, \mathbf{q})$  and  $V_\nu^A(\mathbf{q})$  separately. The  $\mathbf{k}$  integral of (21) produces a delta function which fixes  $\mathbf{b} = \mathbf{b}_2 - \mathbf{b}'_2$ . Introducing  $\mathbf{R} = (\mathbf{b}_2 + \mathbf{b}'_2)/2$  we obtain

$$W_\nu(\mathbf{b}, \mathbf{q}) = \frac{2\pi}{b^2} \int d^2\mathbf{R} e^{+i\mathbf{q}\cdot(\mathbf{R}-\mathbf{b}/2)} \left( \frac{\mathbf{b}^2}{(\mathbf{R}-\mathbf{b}/2)^2 (\mathbf{R}+\mathbf{b}/2)^2} \right)^{1/2-i\nu}. \quad (22)$$

The integral over  $\mathbf{R}$  can be performed using standard Feynman parametrization techniques:

$$W_\nu(\mathbf{b}, \mathbf{q}) = \frac{(2\pi)^2 |\mathbf{b}|}{\Gamma^2(1/2 - i\nu) b^2} \left( \frac{\mathbf{q}^2}{4} \right)^{-i\nu} \int_0^1 dx \frac{e^{-i\mathbf{q}\cdot\mathbf{b}x}}{\sqrt{x(1-x)}} K_{2i\nu}(|\mathbf{q}||\mathbf{b}|\sqrt{x(1-x)}) \quad (23)$$

where  $K_{2i\nu}$  is a modified Bessel function. The  $x$  integral can be performed exactly. In particular, we note that

$$\int_0^1 dx \frac{e^{-i\mathbf{q}\cdot\mathbf{b}x}}{\sqrt{x(1-x)}} K_{2i\nu}(|\mathbf{q}||\mathbf{b}|\sqrt{x(1-x)}) = e^{-i\mathbf{q}\cdot\mathbf{b}/2} \int_0^1 \frac{2dx}{\sqrt{1-x^2}} \cos\left(\frac{1}{2}\mathbf{q}\cdot\mathbf{b}\sqrt{1-x^2}\right) K_{2i\nu}\left(\frac{1}{2}|\mathbf{q}||\mathbf{b}|x\right) \quad (24)$$

and that the right hand side is tabulated in Gradshteyn & Ryzhik [3] (6.737(3)). We find

$$W_\nu(\mathbf{b}, \mathbf{q}) = \frac{2i\pi^4|\mathbf{b}|}{\Gamma^2(1/2 - i\nu) b^2} \left(\frac{\mathbf{q}^2}{4}\right)^{-i\nu} e^{-i\frac{\mathbf{q}\cdot\mathbf{b}}{2}} \Delta_\nu(\mathbf{b}, \mathbf{q}) \quad (25)$$

where

$$\begin{aligned} \Delta_\nu(\mathbf{b}, \mathbf{q}) &= \frac{1}{\sinh 2\pi\nu} \left[ e^{\pi\nu} J_{i\nu} \left( \frac{\sqrt{(\mathbf{q}\cdot\mathbf{b})^2 - \mathbf{q}^2|\mathbf{b}|^2} - \mathbf{q}\cdot\mathbf{b}}{4} \right) J_{i\nu} \left( \frac{\sqrt{(\mathbf{q}\cdot\mathbf{b})^2 - \mathbf{q}^2|\mathbf{b}|^2} + \mathbf{q}\cdot\mathbf{b}}{4} \right) \right. \\ &\quad \left. - (\nu \rightarrow -\nu) \right]. \end{aligned} \quad (26)$$

Equivalently<sup>1</sup>, we have

$$\Delta_\nu(\mathbf{b}, \mathbf{q}) = \frac{2i}{\sinh 2\pi\nu} \text{Im} [J_{i\nu}(bq^*/4) J_{i\nu}(b^*q/4)]. \quad (27)$$

We next turn our attention to  $V_\nu^A(\mathbf{q})$ . This requires some choice for the impact factor  $\Phi_A(\mathbf{k}_1, \mathbf{q})$ . We choose to write the impact factor in the form

$$\Phi_A(\mathbf{k}, \mathbf{q}) = \int d^2\mathbf{r} f_A(\mathbf{r}) \left( e^{i\mathbf{k}\cdot\mathbf{r}/2} - e^{-i\mathbf{k}\cdot\mathbf{r}/2} \right) \left( e^{i(\mathbf{q}-\mathbf{k})\cdot\mathbf{r}/2} - e^{-i(\mathbf{q}-\mathbf{k})\cdot\mathbf{r}/2} \right). \quad (28)$$

This is a general choice, appropriate for scattering off colourless states. Assuming that  $f_A(\mathbf{r}) = f_A(|\mathbf{r}|)$ , the calculation of the function  $V_\nu^A(\mathbf{q})$  can be computed using the method demonstrated in [5]. The result is

$$\begin{aligned} V_\nu^A(\mathbf{q}) &= 2(2\pi)^5 \frac{\Gamma(1/2 - i\nu)}{\Gamma(1/2 + i\nu)} \left(\frac{\mathbf{q}^2}{4}\right)^{-1+i\nu} \int_{1/2-i\infty}^{1/2+i\infty} \frac{dz}{2\pi i} \left\{ \int dr \left(\frac{\mathbf{q}^2\mathbf{r}^2}{16}\right)^z (-f_A(\mathbf{r})) \right. \\ &\quad \frac{\Gamma(1-z-i\nu)}{\Gamma(1/2+z/2-i\nu/2) \Gamma(1-z/2-i\nu/2)} \\ &\quad \left. \frac{\Gamma(1-z+i\nu)}{\Gamma(1/2+z/2+i\nu/2) \Gamma(1-z/2+i\nu/2)} \right\}. \end{aligned} \quad (29)$$

This is a particularly convenient way of expressing  $V_\nu^A$  since it allows the limits  $1/\mathbf{q}^2 \gg \mathbf{r}^2$  and  $1/\mathbf{q}^2 \ll \mathbf{r}^2$  to be extracted with ease (by focusing on the poles lying closest to the contour). Alternatively, we could utilize (24) to write

$$V_\nu^A(\mathbf{q}) = 8i\pi^5 \int d^2\mathbf{r} f_A(\mathbf{r}) |\mathbf{r}| e^{-i\mathbf{q}\cdot\mathbf{r}} \left(\frac{\mathbf{q}^2}{4}\right)^{i\nu} \Delta_\nu(\mathbf{r}, \mathbf{q}). \quad (30)$$

---

<sup>1</sup>We note that this is consistent with the formula given in [4].

This latter form does not assume  $f_A(\mathbf{r}) = f_A(|\mathbf{r}|)$ .

### 3. Inside the BFKL Pomeron

We are now in a position to investigate the typical distances involved in the exchange. We can “look inside” the Pomeron and examine its size at some intermediate rapidity,  $y'$ . The probability density for having a Pomeron with size  $|\mathbf{b}|$  at rapidity  $y'$  is proportional to the product of the wavefunctions,  $\Psi_A(y', \mathbf{b}, \mathbf{q})\Psi_B^*(y - y', \mathbf{b}, \mathbf{q})$  (see (18)). We need to make some assumption regarding the nature of the external states in order to deduce the process dependent  $V_\nu^A$ . We work with (29) under the assumption that the external state is characterised by a single scale,  $Q$ . In this case, we can write

$$\int_0^\infty dr \left( \frac{\mathbf{q}^2 r^2}{16} \right)^z (-f(r)) = Q \left( \frac{\mathbf{q}^2}{16Q^2} \right)^z h(z) \quad (31)$$

where  $h(z)$  is some dimensionless function of  $z$  which contains poles only to the left of the  $z$  plane contour,  $\text{Re } z = 1/2$ , otherwise the impact factor  $\Phi_A$  is not defined. For photon and vector meson external states the following expressions for  $h(z)$  are needed:

$$\begin{aligned} -f(r) = Q^2 K_0(Qr) &\Rightarrow h(z) = 2^{2z-1} \Gamma^2(1/2 + z) \\ -f(r) = Q^2 K_1(Qr) &\Rightarrow h(z) = 2^{2z-1} \Gamma(1 + z) \Gamma(z). \end{aligned} \quad (32)$$

By way of example we also note that

$$\begin{aligned} -f(r) = \frac{Q}{r} e^{-Q^2 r^2} &\Rightarrow h(z) = \frac{\Gamma(z)}{2} \\ -f(r) = r Q^3 e^{-Q^2 r^2} &\Rightarrow h(z) = \frac{\Gamma(1 + z)}{2} \\ -f(r) = \delta(r^2 - 1/Q^2) &\Rightarrow h(z) = 1/2. \end{aligned} \quad (33)$$

The existence of double poles induces additional logarithms in the final answer but does not affect any of our main conclusions. Subsequently, we will therefore assume that  $h(z)$  contains only single poles. We can now proceed to examine the wavefunction in the limits  $\mathbf{q}^2 \ll Q^2$  and  $\mathbf{q}^2 \gg Q^2$ .

#### The case when $\mathbf{q}^2 < 16 Q^2$

In this case the  $z$ -plane contour of (29) can be closed in the right half plane. We consequently pick up the poles in  $V_\nu^A$  which come from the process independent part, i.e. at  $z = 1 \pm i\nu$ . Evaluating the integral keeping only the nearest pole gives

$$\begin{aligned} V_\nu(\mathbf{q}) = & \frac{2(2\pi)^5 Q}{\sqrt{\pi}} \frac{\Gamma(1/2 - i\nu)}{\Gamma(1/2 + i\nu)} \left( \frac{\mathbf{q}^2}{4} \right)^{-1+i\nu} \left[ \left( \frac{\mathbf{q}^2}{16Q^2} \right)^{1+i\nu} \frac{h(1 + i\nu) \Gamma(-2i\nu)}{\Gamma(1/2 - i\nu) \Gamma(1 + i\nu)} \right. \\ & \left. + \left( \frac{\mathbf{q}^2}{16Q^2} \right)^{1-i\nu} \frac{h(1 - i\nu) \Gamma(2i\nu)}{\Gamma(1/2 + i\nu) \Gamma(1 - i\nu)} \right]. \end{aligned} \quad (34)$$

The corrections to this expression are suppressed by powers of  $\mathbf{q}^2/Q^2$ . We have only the  $\nu$  integral to perform in order to obtain the wavefunction  $\Psi_A$ . In order to proceed further we consider the two regions  $|\mathbf{q}| > 1/|\mathbf{b}|$  and  $|\mathbf{q}| < 1/|\mathbf{b}|$  separately.

In the region where  $|\mathbf{q}||\mathbf{b}| \lesssim 1$  we can use the small argument expansions of the Bessel functions, and for large  $y$  the dominant contribution to the  $\nu$  integral in (19) will come from the region of small  $\nu$ , hence we may write

$$W_\nu(\mathbf{b}, \mathbf{q}) \approx \frac{(2\pi)^2 |\mathbf{b}|}{2\nu b^2} \left( \frac{\mathbf{q}^2}{4} \right)^{-i\nu} \sin\left(\nu \ln(16/(\mathbf{q}^2 \mathbf{b}^2))\right). \quad (35)$$

Whilst for  $V_\nu$  the corresponding small  $\nu$  limit of (34) is

$$V_\nu^A(\mathbf{q}) \approx \frac{16h(1)\pi^4}{Q\nu} \left( \frac{\mathbf{q}^2}{4} \right)^{i\nu} \sin\left(\nu \ln(16Q^2/\mathbf{q}^2)\right). \quad (36)$$

For the wavefunction, we thus obtain

$$\Psi_A(y, \mathbf{b}, \mathbf{q}) \approx 8h(1) \frac{|\mathbf{b}|}{Qb^2} \int d\nu e^{\bar{\alpha}_S \chi(\nu)y} \sin\left(\nu \ln(16/(\mathbf{q}^2 \mathbf{b}^2))\right) \sin\left(\nu \ln(16Q^2/\mathbf{q}^2)\right). \quad (37)$$

Expanding the BFKL eigenfunction about  $\nu = 0$  allows the integral to be performed. Using  $\chi(\nu) \approx 4 \ln 2 - 14\zeta(3)\nu^2$  yields

$$\Psi_A(y, \mathbf{b}, \mathbf{q}) = 4\sqrt{\pi}h(1) \frac{|\mathbf{b}|}{Qb^2} \frac{e^{\omega_0 y}}{(a^2 y)^{1/2}} \left[ \exp\left(\frac{-\ln^2(\mathbf{b}^2 Q^2)}{4a^2 y}\right) - \exp\left(\frac{-\ln^2(256Q^2/(\mathbf{q}^4 \mathbf{b}^2))}{4a^2 y}\right) \right]. \quad (38)$$

Here  $a^2 = 14\bar{\alpha}_S \zeta(3)$ .

In the region where  $|\mathbf{q}||\mathbf{b}| \gg 1$  the function  $V_\nu^A$  is again given by (36). For  $W_\nu$  we take the large argument approximation to the Bessel functions. After some algebra we find that

$$W_\nu(\mathbf{b}, \mathbf{q}) \simeq \frac{(2\pi)^2}{|\mathbf{q}|b^2} \left( \frac{\mathbf{q}^2}{4} \right)^{-i\nu} (1 + e^{-i\mathbf{q}\cdot\mathbf{b}}). \quad (39)$$

Inserting (36) and (39) into our expression for  $\Psi_A$  (19) yields

$$\Psi_A(y, \mathbf{b}, \mathbf{q}) \approx \frac{16h(1)}{Q|\mathbf{q}|b^2} (1 + e^{-i\mathbf{q}\cdot\mathbf{b}}) \int d\nu e^{\bar{\alpha}_S \chi(\nu)y} \nu \sin\left(\nu \ln(16Q^2/\mathbf{q}^2)\right) \quad (40)$$

which evaluates (on expanding the eigenvalue) to

$$\Psi_A(y, \mathbf{b}, \mathbf{q}) = \frac{8h(1)\sqrt{\pi}}{Q|\mathbf{q}|b^2} (1 + e^{-i\mathbf{q}\cdot\mathbf{b}}) \frac{e^{\omega_0 y}}{(a^2 y)^{3/2}} \ln(16Q^2/\mathbf{q}^2) \exp(-\ln^2(16Q^2/\mathbf{q}^2)/4a^2 y). \quad (41)$$

Note that in the limit  $\mathbf{q} \rightarrow 0$  we only have the region described by (38) in which the second exponential term vanishes. This corresponds to the well known result for diffusion about the size of the external state,  $Q$ . In that case there is nothing to prevent diffusion into the large



distance region where a perturbative calculation may be unreliable. (see, e.g. [6] for a more detailed study of diffusion at  $t = 0$ .) However, the effect of a finite  $\mathbf{q}^2$  is dramatic. Equation (41) reveals that there is no diffusion inside the region  $|\mathbf{b}||\mathbf{q}| > 1$ . Moreover, the distribution in this region vanishes rapidly as  $\mathbf{b}$  increases. The result is that diffusion to large sizes is effectively blocked beyond the scale  $1/|\mathbf{q}|$  [7]. The momentum transfer acts as an effective infrared cut-off. In Fig. 3 we illustrate the diffusion for the case  $\mathbf{q} = 0$ . This should be compared with Fig. 4 in which we show the equivalent distributions for the case  $\mathbf{q}^2 = 1 \text{ GeV}^2$ . In generating these plots we chose a simple Gaussian form for the function  $f(r)$  which characterises the external impact factor,  $|f(r)| = Q/re^{-Q^2r^2}$ . As we noted earlier this corresponds to a function  $h(z) = \Gamma(z)/2$ .

### The case when $\mathbf{q}^2 > 16 Q^2$

For this case the  $z$ -plane contour integral must be closed in the left half plane. The only poles are those which arise from the process dependent factor  $h(z)$ . In the limit  $\mathbf{q}^2 \gg 16 Q^2$  the rightmost pole gives the leading power dependence. If this is a single pole at  $z = -z_0$  then we can take

$$h(z) \approx \frac{h_L(z)}{z + z_0}. \quad (42)$$

We can now evaluate  $V_\nu^A$ :

$$\begin{aligned} V_\nu(\mathbf{q}) = & 2(2\pi)^5 \frac{\Gamma(1/2 - i\nu)}{\Gamma(1/2 + i\nu)} \left(\frac{\mathbf{q}^2}{4}\right)^{-1+i\nu} Q h_L(-z_0) \left(\frac{16Q^2}{\mathbf{q}^2}\right)^{z_0} \\ & \frac{\Gamma(1 - z_0 - i\nu)}{\Gamma(1/2 + z_0/2 - i\nu/2) \Gamma(1 - z_0/2 - i\nu/2)} \\ & \frac{\Gamma(1 - z_0 + i\nu)}{\Gamma(1/2 + z_0/2 + i\nu/2) \Gamma(1 - z_0/2 + i\nu/2)}. \end{aligned} \quad (43)$$

The corrections are suppressed by powers of  $Q^2/\mathbf{q}^2$ . We can again separate the analysis into two regions consisting of large and small  $|\mathbf{q}||\mathbf{b}|$ .

In the region where  $|\mathbf{q}||\mathbf{b}| \lesssim 1$  the function  $W_\nu(\mathbf{b}, \mathbf{q})$  is again given by (35). For  $V_\nu$  the corresponding small  $\nu$  limit of (43) is

$$V_\nu^A(\mathbf{q}) \approx 64\pi^4 \left(\frac{\mathbf{q}^2}{4}\right)^{-1+i\nu} \left(\frac{64Q^2}{\mathbf{q}^2}\right)^{z_0} Q \tilde{h}_L(z_0). \quad (44)$$

where we have further defined

$$\tilde{h}_L(z_0) = h_L(-z_0) \left(\frac{\Gamma(1/2 + z_0/2)}{\Gamma(1/2 - z_0/2)}\right)^2. \quad (45)$$

This form is only appropriate providing  $z_0$  does not induce poles in the denominator, i.e.  $z_0$  is not an odd integer. Although it would be straightforward to accommodate such values of  $z_0$  (since they merely produce an additional factor of  $\nu^2$  in the numerator) we shall ignore this

possibility in the following. This does not affect our main conclusions. For the wavefunction, we now obtain

$$\Psi_A(y, \mathbf{b}, \mathbf{q}) \approx 128 \tilde{h}_L(z_0) \frac{Q|\mathbf{b}|}{b^2 \mathbf{q}^2} \left( \frac{64Q^2}{\mathbf{q}^2} \right)^{z_0} \int d\nu \nu e^{\bar{\alpha}_S \chi(\nu)y} \sin\left(\nu \ln(16/(\mathbf{q}^2 \mathbf{b}^2))\right). \quad (46)$$

Expanding the BFKL eigenfunction about  $\nu = 0$  gives

$$\Psi_A(y, \mathbf{b}, \mathbf{q}) = 64\sqrt{\pi} \tilde{h}_L(z_0) \frac{Q|\mathbf{b}|}{b^2 \mathbf{q}^2} \left( \frac{64Q^2}{\mathbf{q}^2} \right)^{z_0} \frac{e^{\omega_0 y}}{(a^2 y)^{3/2}} \ln(16/(\mathbf{q}^2 \mathbf{b}^2)) \exp\left(\frac{-\ln^2(16/(\mathbf{q}^2 \mathbf{b}^2))}{4a^2 y}\right). \quad (47)$$

In the region where  $|\mathbf{q}||\mathbf{b}| \gg 1$  the function  $V_\nu^A$  is again given by (44) whilst  $W_\nu(\mathbf{b}, \mathbf{q})$  is given by (39). Inserting (44) and (39) into our expression for  $\Psi_A$  (19) yields

$$\Psi_A(y, \mathbf{b}, \mathbf{q}) \approx 256 \frac{Q}{|\mathbf{q}|^3 b^2} \tilde{h}_L(z_0) \left( \frac{64Q^2}{\mathbf{q}^2} \right)^{z_0} (1 + e^{-i\mathbf{q}\cdot\mathbf{b}}) \int d\nu \nu^2 e^{\bar{\alpha}_S \chi(\nu)y} \quad (48)$$

which evaluates (on expanding the eigenvalue) to

$$\Psi_A(y, \mathbf{b}, \mathbf{q}) = 128\sqrt{\pi} \frac{Q}{|\mathbf{q}|^3 b^2} \tilde{h}_L(z_0) \left( \frac{64Q^2}{\mathbf{q}^2} \right)^{z_0} (1 + e^{-i\mathbf{q}\cdot\mathbf{b}}) \frac{e^{\omega_0 y}}{(a^2 y)^{3/2}}. \quad (49)$$

Notice that the wavefunction of (47) corresponds to diffusion about  $\mathbf{b}^2 = 16/\mathbf{q}^2$ , i.e. the diffusion is no longer centred around the external scale,  $Q$ , determined by the impact factor. As before the momentum transfer  $\mathbf{q}$  acts as an effective infrared cut-off. These properties can be seen in Fig. 5

The wavefunction  $\Psi_B^*$  can be computed analogously. For the sake of illustration, we shall assume that the external states,  $A$  and  $B$ , are defined in terms of the scales  $Q_A$  and  $Q_B$  respectively and that in all other respects they are equal. In this case,  $\Psi_B^*$  is simply the complex conjugate of  $\Psi_A$  with  $Q_A$  replaced by  $Q_B$ . Note that the complex factors in the denominators always combine to produce the factor  $1/\mathbf{b}^4$  in the probability density ( $= \Psi_A \Psi_B^*$ ). We shall evaluate the probability distribution  $\Psi_A \Psi_B^*$  for three separate cases. Firstly, when the external scales ( $Q_A$  and  $Q_B$ ) are both larger than the momentum transfer; secondly, when one is large and one is small and finally when both are small.

In Figures 6,7 and 8, we show the width of the  $b$ -distribution as a function of  $y'$ . The width is determined by evaluating the value of  $\ln \mathbf{b}$  when  $\mathbf{b}^2 \Psi_A \Psi_B^*$  is half of its maximum. Since

$$\frac{A(s, t)}{s} \sim \int d(\ln \mathbf{b}^2) \mathbf{b}^2 \Psi_A(y', \mathbf{b}, \mathbf{q}) \Psi_B^*(y - y', \mathbf{b}, \mathbf{q}) \quad (50)$$

it follows that for the dominance of short distance physics the ‘‘cigar’’ must remain inside the region of small  $|\mathbf{b}|$ . Fig. 6 shows the case when both external scales are larger than the momentum transfer,  $\mathbf{q}^2$ . In this case the diffusion is similar to the  $\mathbf{q}^2 = 0$  case, i.e. increasingly larger distances are probed as  $y'$  approaches  $y/2$ . However, movement to distances larger than  $\sim 1/|\mathbf{q}|$  is blocked. This (almost) total exclusion from the region  $|\mathbf{b}| \gtrsim 1/|\mathbf{q}|$  remains even if

one or both of the external scales becomes small. In these cases the picture is quite different from the  $\mathbf{q}^2 = 0$  case. Fig. 7 shows the diffusion when one external scale is large and the other is small. The case where both external scales are smaller than the momentum transfer,  $\mathbf{q}^2$  is shown in Fig. 8.

**Acknowledgements:** We thank Jochen Bartels, Hans Lotter, Douglas Ross, Misha Ryskin and Mark Wüsthoff for numerous helpful discussions.

## References

- [1] E.A.Kuraev, L.N.Lipatov & V.S.Fadin, Sov.Phys.JETP **44** (1976) 443; Sov.Phys.JETP **45** (1977) 199; I.I.Balitsky & L.N.Lipatov, Sov.J.Nucl.Phys. **28** (1978) 822.
- [2] L.N.Lipatov, Sov.Phys.JETP **63** (1986) 904.
- [3] I.S.Gradshcheyn & I.M.Ryzhik, “Table of Integrals, Series and Products”, 5th Edition, Academic Press (1994).
- [4] H.Navelet & R.Peschanski, “Conformal blocks in the QCD Pomeron formalism”, hep-ph/9611396.
- [5] J.Bartels, J.R.Forshaw, H.Lotter & M.Wusthoff, Phys.Lett. **B375** (1996) 301.
- [6] J.Bartels & H.Lotter, Phys.Lett. **B309** (1993) 400.
- [7] H.Lotter, “Numerische Simulation der BFKL Evolution in Prozessen der Assoziierten Jet-Produktion”, Diplomarbeit, Universität Hamburg (1993).

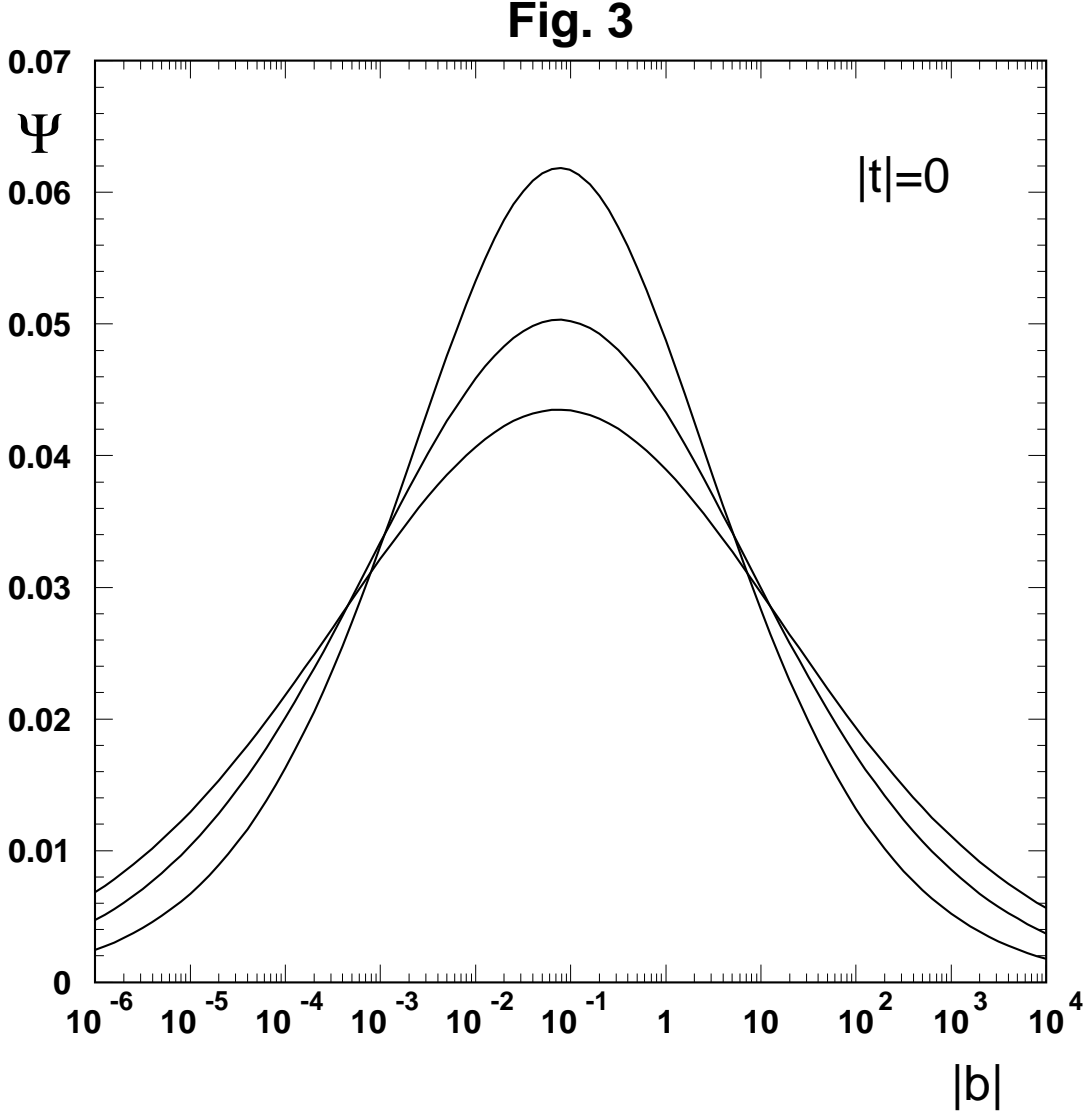


Figure 3: The distribution of gluon size inside the BFKL Pomeron for  $|t| = \mathbf{q}^2 = 0$  and  $Q = 10$  GeV as described by  $\Psi = \Psi_A b^2/|\mathbf{b}|$ . The plot shows the broadening of the distribution as the rapidity,  $y$ , is increased through the values  $y = 10, 15$  and  $20$ . Nothing prevents diffusion into the long distance region. The curves are from a numerical calculation of (19) using (25) and (29). Each curve has been scaled by a factor  $e^{-\omega_0 y}$ .

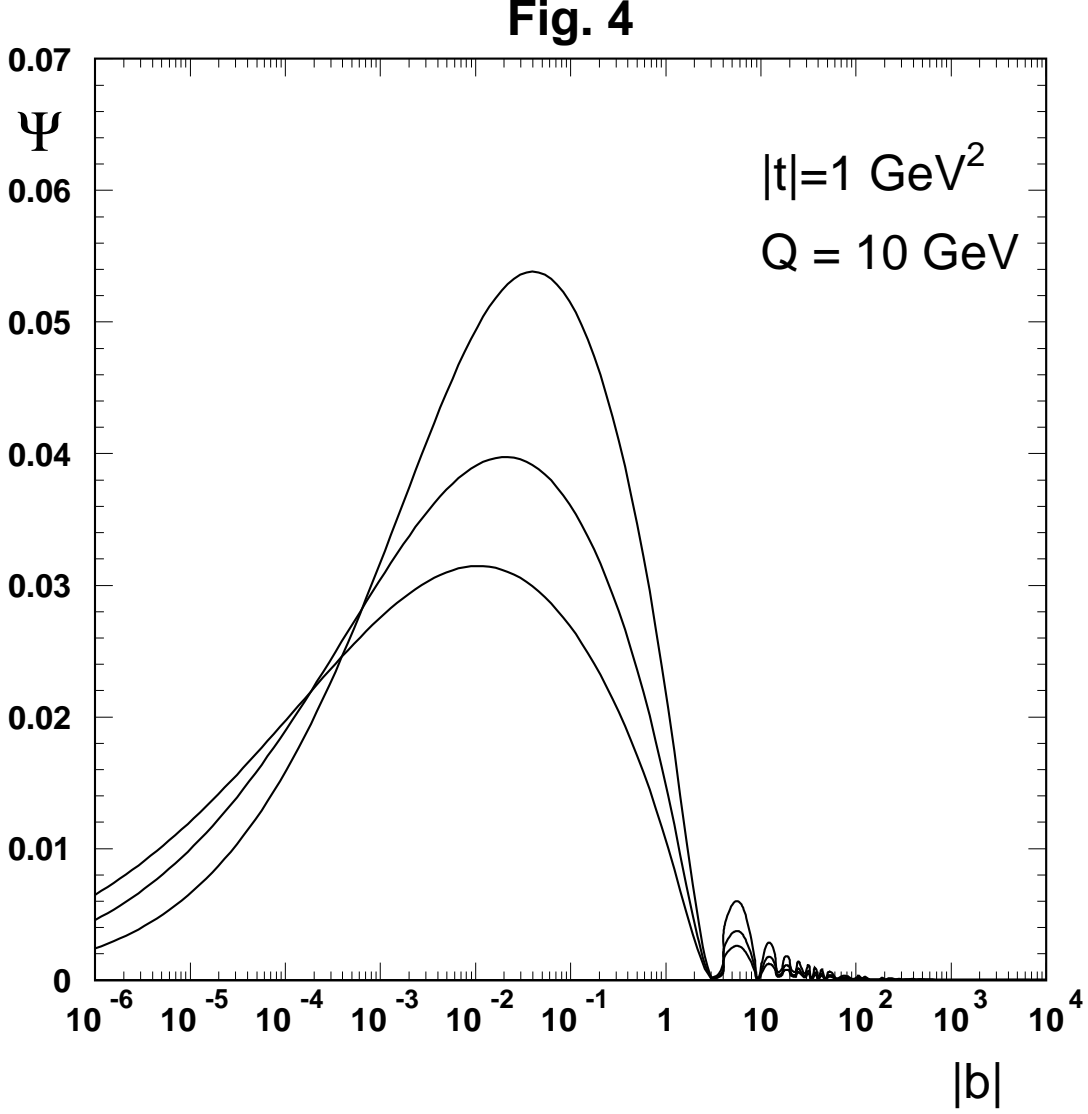


Figure 4: The distribution of gluon size inside the BFKL Pomeron for  $|t| = \mathbf{q}^2 = 1 \text{ GeV}^2$  and  $Q = 10 \text{ GeV}$  as described by  $\Psi = \Psi_A b^2/|\mathbf{b}|$ . The plot shows the broadening of the distribution as the rapidity,  $y$ , is increased through the values  $y = 10, 15$  and  $20$ . The scale  $\mathbf{q}$  acts as an effective infrared cut off preventing diffusion into the infrared region. The curves are from a numerical calculation of (19) using (25) and (29). Each curve has been scaled by a factor  $e^{-\omega_0 y}$ .

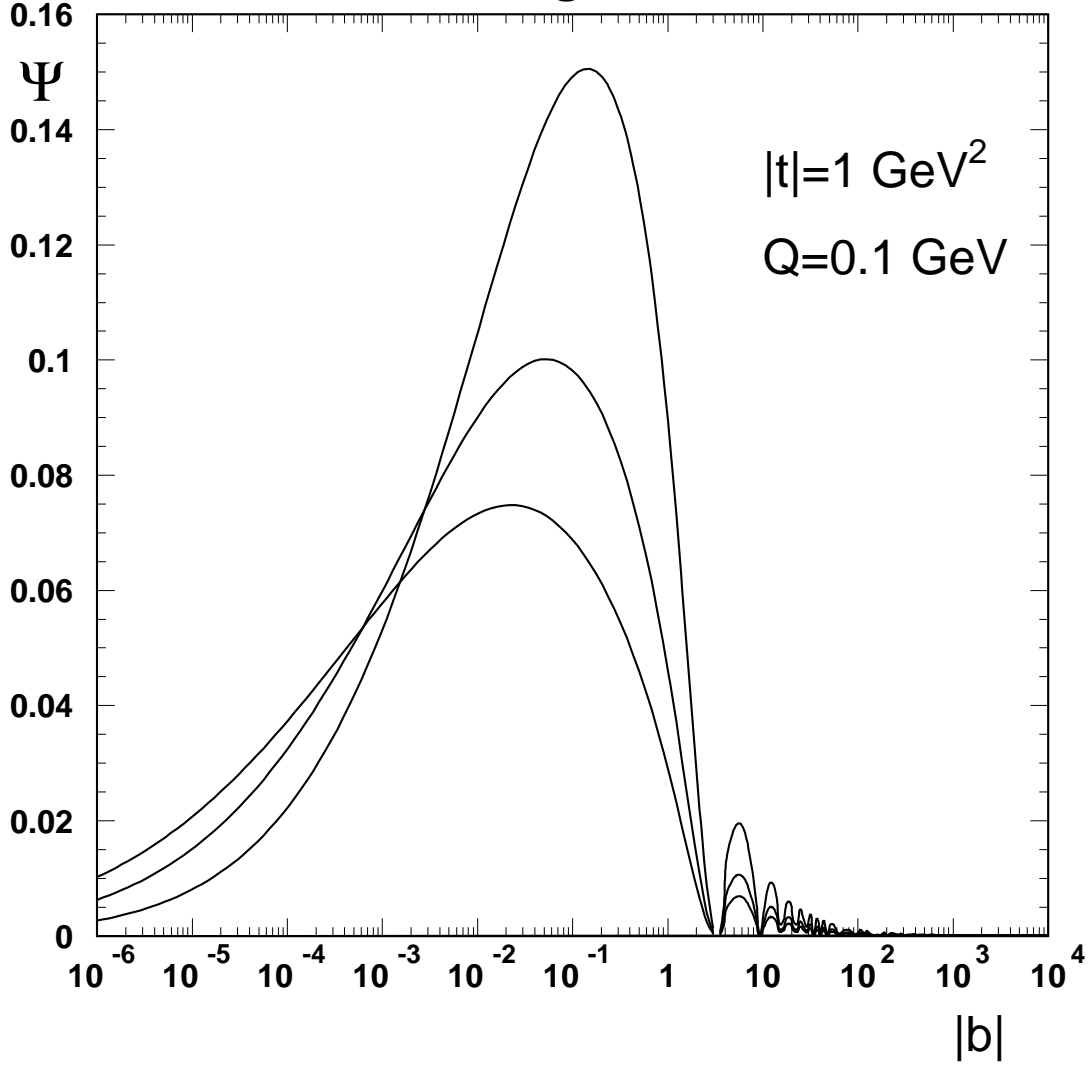
**Fig. 5**

Figure 5: The distribution of gluon size inside the BFKL Pomeron for  $|t| = \mathbf{q}^2 = 1 \text{ GeV}^2$  and  $Q = 0.1 \text{ GeV}$  as described by  $\Psi = \Psi_A b^2/|\mathbf{b}|$ . The plot shows the broadening of the distribution as the rapidity,  $y$ , is increased through the values  $y = 10, 15$  and  $20$ . The scale  $\mathbf{q}$  acts as an effective infrared cut off preventing diffusion into the infrared region. The curves are from a full numerical calculation of (19) using (25) and (29). Each curve has been scaled by a factor  $e^{-\omega_0 y}$ .

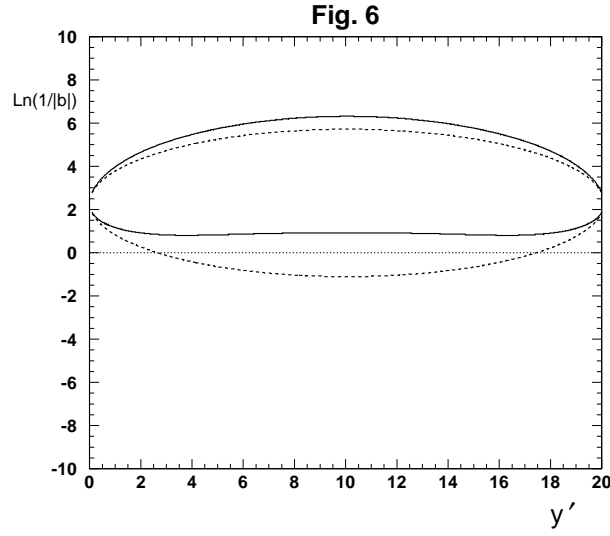


Figure 6: The width (as defined by half the maximum) of the distribution  $\mathbf{b}^2\Psi_A\Psi_B^*$  for the case  $Q_A = Q_B = 10$  GeV and  $y = 20$ . The dotted lines represent the  $|t| = 0$  case. The full lines represent the case  $|t| = \mathbf{q}^2 = 1$  GeV<sup>2</sup>.

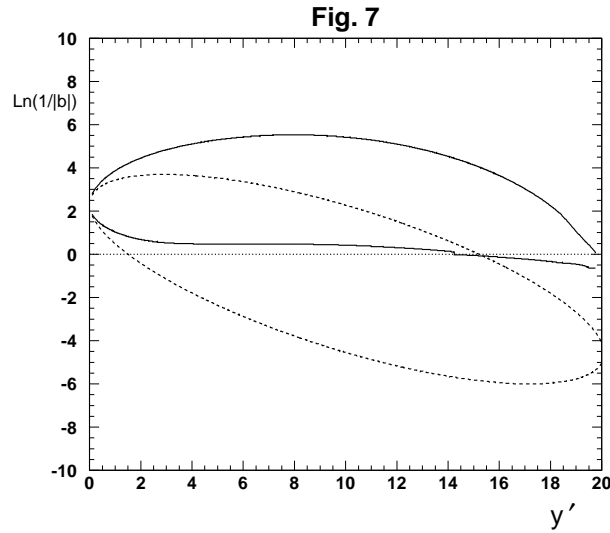


Figure 7: The width (as defined by half the maximum) of the distribution  $\mathbf{b}^2\Psi_A\Psi_B^*$  for the case  $Q_A = 10$  GeV,  $Q_B = 10^{-2}$  GeV and  $y = 20$ . The dotted lines represent the  $|t| = 0$  case. The full lines represent the case  $|t| = \mathbf{q}^2 = 1$  GeV<sup>2</sup>.

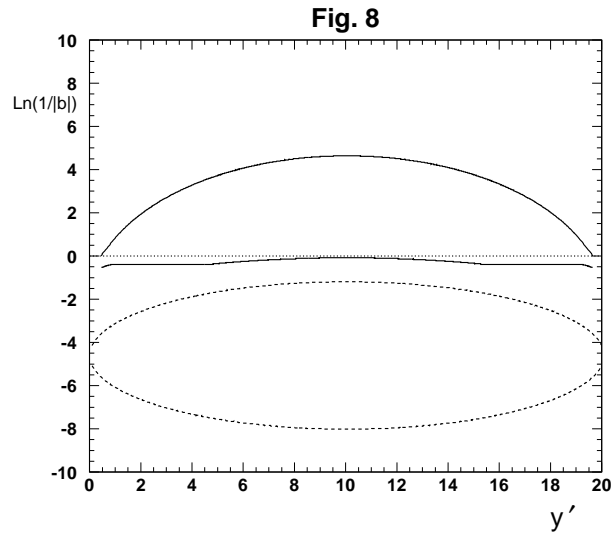


Figure 8: The width (as defined by half the maximum) of the distribution  $\mathbf{b}^2\Psi_A\Psi_B^*$  for the case  $Q_A = Q_B = 10^{-2} \text{ GeV}$  and  $y = 20$ . The dotted lines represent the  $|t| = 0$  case. The full lines represent the case  $|t| = \mathbf{q}^2 = 1 \text{ GeV}^2$ .